



Original article

Treating locally advanced lung cancer with a 1.5 T MR-Linac – Effects of the magnetic field and irradiation geometry on conventionally fractionated and isotoxic dose-escalated radiotherapy

Hannah E. Bainbridge^{a,b,*,1}, Martin J. Menten^{c,1}, Martin F. Fast^c, Simeon Nill^c, Uwe Oelfke^{c,2}, Fiona McDonald^{a,b,2}^a Department of Radiotherapy at The Royal Marsden NHS Foundation Trust; ^b The Institute of Cancer Research; and ^c Joint Department of Physics at The Institute of Cancer Research and The Royal Marsden NHS Foundation Trust, London, United Kingdom

ARTICLE INFO

Article history:

Received 28 April 2017

Received in revised form 21 August 2017

Accepted 9 September 2017

Available online xxxx

Keywords:

MRI-guided radiotherapy

Lung cancer

MR-Linac

Dose-escalation

ABSTRACT

Purpose: This study investigates the feasibility and potential benefits of radiotherapy with a 1.5 T MR-Linac for locally advanced non-small cell lung cancer (LA NSCLC) patients.**Material and methods:** Ten patients with LA NSCLC were retrospectively re-planned six times: three treatment plans were created according to a protocol for conventionally fractionated radiotherapy and three treatment plans following guidelines for isotoxic target dose escalation. In each case, two plans were designed for the MR-Linac, either with standard (~7 mm) or reduced (~3 mm) planning target volume (PTV) margins, while one conventional linac plan was created with standard margins. Treatment plan quality was evaluated using dose–volume metrics or by quantifying dose escalation potential.**Results:** All generated treatment plans fulfilled their respective planning constraints. For conventionally fractionated treatments, MR-Linac plans with standard margins had slightly increased skin dose when compared to conventional linac plans. Using reduced margins alleviated this issue and decreased exposure of several other organs-at-risk (OAR). Reduced margins also enabled increased isotoxic target dose escalation.**Conclusion:** It is feasible to generate treatment plans for LA NSCLC patients on a 1.5 T MR-Linac. Margin reduction, facilitated by an envisioned MRI-guided workflow, enables increased OAR sparing and isotoxic target dose escalation for the respective treatment approaches.© 2017 The Authors. Published by Elsevier Ireland Ltd. Radiotherapy and Oncology xxx (2017) xxx–xxx
This is an open access article under the CC BY-NC-ND license (<http://creativecommons.org/licenses/by-nc-nd/4.0/>).

Current survival rates for patients with locally advanced non-small cell lung cancer (LA NSCLC) are poor [1,2]. In spite of improvements in both radiotherapy technology and systemic therapies, some suggest that current treatment strategies have reached their therapeutic ceiling [3]. Effective local disease control is essential for the survival of these patients [1]. Taking heed from stereotactic radiotherapy for early-stage NSCLC patients, where biologically equivalent doses of 100 Gy and more result in local disease control rates greater than 90% [4], dose intensification continues to be investigated in LA NSCLC patients. Indiscriminate target dose escalation, delivered with a prolonged overall treatment

course, may be detrimental [5,6]. However, data have shown promising outcomes in LA NSCLC patients treated with accelerated isotoxic dose-escalated radiotherapy [7–11], where each patient was prescribed an individualized target dose, escalated on the basis of normal-tissue tolerances up to a trial-specific maximum target dose [3].

During a course of radical radiotherapy for LA NSCLC patients, there can be substantial inter- and intra-fractional changes in thoracic anatomy, due to respiratory and cardiac motion, patient weight loss, tumour growth or shrinkage, or changes in the surrounding lung [12,13]. Daily cone-beam CT scans are utilized to set patients up according to the observed tumour position and any remaining uncertainties are accounted for using planning target volume (PTV) margins. However, large margins result in increased irradiation of healthy tissue and restrict isotoxic target dose escalation.

Recently, MRI-guided treatment units have emerged, allowing acquisition of MR images immediately prior to and during

* Corresponding author at: Institute of Cancer Research, 15 Cotswold Road, Sutton SM2 5NG, United Kingdom.

E-mail addresses: Hannah.bainbridge@icr.ac.uk (H.E. Bainbridge), martin.menten@icr.ac.uk (M.J. Menten).

¹ Joint first authors.

² Joint last authors.

radiotherapy delivery [14–17]. The availability of these images with improved soft-tissue contrast may increase target delineation reproducibility, as has been shown for other tumour sites, and reduce setup uncertainties [18–20]. Integrating MRI-guided units into clinical practice has implications for treatment planning as treatments will be delivered within a static magnetic field. These differ from the ones delivered at zero magnetic field because the trajectories of secondary electrons are altered by the Lorentz force [21,22] and may cause local increases in dose (“hot spots”), especially at air-tissue-interfaces, where electrons can loop around and deposit energy at the surface they have been ejected from [23]. Furthermore, the irradiation geometry and beam energy of MRI-guided units deviate from the ones realized for conventional linacs.

Several studies have evaluated the effect of magnetic fields and irradiation geometry on stereotactic radiotherapy of early-stage NSCLC [24–29]. However, none have specifically investigated the use of MRI-guided units for treatment of patients with LA NSCLC. This study used an isotoxic dose-escalated trial protocol as well as a conventionally fractionated scheme to generate treatment plans for a conventional linac and plans for a 1.5 T MR-Linac using standard or reduced margins. By comparing the planned dose distributions we explored the hypothesis that it is feasible to create clinically acceptable radiotherapy plans for the MR-Linac. Furthermore, the effect of reducing PTV margins with regard to sparing of healthy tissue and potential target dose escalation was investigated.

Material and methods

Patient datasets and contouring

For this study we used treatment planning 4DCT scans of ten consecutive patients undergoing radical radiotherapy for LA NSCLC at our institution. The scans were acquired using a Philips Brilliance CT Big Bore scanner (Philips Medical Systems, Best, the Netherlands) with a voxel size of $\sim 1 \times 1 \times 2 \text{ mm}^3$. Details of the patient characteristics can be found in the [Supplemental material](#). All patients had given written, informed consent for their scans to be used for research purposes.

One clinician contoured the gross tumour volume (GTV) on each of the ten phases of the 4DCT scan. In order to account for microscopic disease spread, each GTV contour was expanded isotropically by 5 mm to derive the clinical target volumes (CTV). Afterwards, the union of the CTV contours was used to create the internal target volume (ITV) on the average CT image, which was derived from the 4D acquisition.

Two different margin approaches were used to calculate the planning target volume (PTV). Standard PTV margins expanded the ITV by approximately 7 mm, depending on direction, and emulate the clinical standard at our institution. A smaller PTV using reduced margins of approximately 3 mm was also created. This was motivated by the potential reduction of treatment uncertainties with the envisioned MR-Linac workflow that would incorporate patient imaging, delineation of critical structures and adaptation of the treatment plan before each fraction [30]. We assume that the use of MR images with high soft-tissue contrast allows for more accurate target delineation and localization. Additionally, a future MR-Linac workflow could potentially incorporate plan re-optimization for each fraction and allow adaptation of the ITV to inter-fractional changes in tumour motion magnitude. Both PTV margins were calculated using van Herk's margin recipe and [Table 1](#) summarizes the individual error contributions, which were either derived from clinical judgment or taken from the literature [31,32]. While this approach disregards the contouring accuracy on MR images depending on the position of the tumour relative

to other soft tissues, a revision of the margin concept is beyond the scope of this study.

The mediastinal envelope, heart, oesophagus, brachial plexus, spinal canal, skin and lungs were delineated on the average CT image. The lung structure was defined as both lungs minus the union of all GTV contours. The skin was defined as the 5 mm rind of the patient contour.

Treatment planning technique and machine models

All treatment plans were designed using the Monaco treatment planning system (Elekta AB, Stockholm, Sweden), research version 5.19.02. Monaco allows for treatment plan optimization and dose calculation under consideration of the magnetic field. Its dose calculation also accounts for the irradiation geometry of the prototype of the 1.5 T MR-Linac, such as the specific beam energy, beam filtration, fixed isocenter, source-to-axis distance and the MLC leaf width at isocenter. Key differences to the conventional Elekta Versa HD linac are provided in [Table 2](#).

For each patient case, we designed treatment plans following two different protocols. One set of plans was designed according to a conventional fractionation protocol with 55 Gy in 20 fractions. The other plans were created based on the United Kingdom isotoxic intensity modulated radiotherapy (IMRT) trial protocol that allows for isotoxic target dose escalation up to 79.2 Gy in 44 fractions (treating twice daily) by increasing the number of 1.8 Gy fractions until an organ-at-risk (OAR) constraint is reached [33]. For this study, we adapted the protocol and removed the artificial limit on maximum target prescription dose. Planning guidelines for both protocols can be found in the [Supplemental material](#). For each of the two planning approaches, three plans were generated: one for the conventional Versa HD linac without a beam flattening filter and two for the MR-Linac. Treatment plans for the MR-Linac were designed with either standard or reduced PTV margins, whereas plans for the conventional linac were generated using standard PTV margins.

All plans were generated using step-and-shoot IMRT with nine equidistant, coplanar beams. The beam isocenter was positioned at the centre of the ITV for the conventional linac treatment plans and fixed at the centre of the MR bore, 13 cm above the treatment couch's surface for the MR-Linac plans. In order to ensure comparability of all plans, the plans were scaled so that the mean ITV dose was equal to the respective prescription level. Additionally, we used similar optimization functions and equal plan modulation options for all treatment plans per respective treatment protocol. All dose distributions were calculated as dose-to-medium dose using Elekta's Monte Carlo engine based on work by Hissoiny et al. [34] with a statistical dose uncertainty of 2% per calculation on a dose grid of $0.25 \times 0.25 \times 0.25 \text{ cm}^3$.

Plan evaluation

For each patient, the dose to OAR and potential for target dose escalation calculated for the conventional linac was compared to that for the MR-Linac with standard margins to investigate the effect of the different irradiation geometries. Similarly, plans for the conventional linac were compared to those for the MR-Linac with reduced margins to assess the effect of additional margin reduction.

Conventionally fractionated plans were compared by evaluating differences in several dose–volume metrics. Statistical significance of the differences was evaluated with a paired *t*-test after confirming normal distribution using Lilliefors test [35]. Five metrics of primary interest were chosen on a *pre-hoc* basis, because they either have been shown to be associated with treatment toxicity, they are highly influential during plan optimization or because of

Table 1

Components contributing to the standard or reduced margins in left–right (LR), superior–inferior (SI) or anterior–posterior (AP) direction. Margins were calculated to ensure coverage of 90% of the target volume with the prescription dose for 90% of patient population.

	Conventional linac workflow/standard margins [mm]			MR-Linac workflow/reduced margins [mm]		
	LR	SI	AP	LR	SI	AP
Contouring error	2.0	2.0	2.0	1.0	1.0	1.0
Difference in observed 4D tumour motion between planning and fraction	1.2	1.6	1.4	–	–	–
Total systematic error	2.3	2.6	2.4	1.0	1.0	1.0
Intrafractional baseline drift	1.5	1.7	1.8	1.5	1.7	1.8
Per-fraction localization error	2.0	2.0	2.0	1.0	1.0	1.0
Total random error	2.5	2.6	2.7	1.8	2.0	2.1
Beam penumbra	6.4	6.4	6.4	8.0	8.0	8.0
Total margin	6.4	7.1	6.8	2.8	2.9	2.9

Table 2

Notable differences in irradiation geometry between a conventional Versa HD linac and the MR-Linac prototype, currently being developed by Elekta.

	Versa HD	MR-Linac prototype
Static magnetic field	–	1.5 T
Nominal beam energy	6 MV	7 MV
Additional beam filtration	–	Cryostat
Source-to-axis distance	100.0 cm	142.5 cm
MLC leaf width at isocenter	5.0 mm	7.15 mm
Isocenter position relative to patient	Variable	Fixed at bore centre

their potential sensitivity to the presence of the 1.5 T magnetic field: Mean lung dose, the percentage volume of the lung receiving 17 Gy or more (lung $V_{17\text{Gy}}$), which is derived from the $V_{20\text{Gy}}$ metric in treatments with 2 Gy fractions, oesophagus $V_{30\text{Gy}}$, heart $V_{25\text{Gy}}$ and the maximum dose received by 2% of contoured skin (skin $D_{2\%}$). The statistical significance level for these metrics was chosen to be $p = 0.01$ after correcting for multiple testing using a Bonferroni correction for a level of $p = 0.05$ [36]. An array of other dose–volume metrics was investigated in an exploratory analysis with a significance level of $p = 0.05$ without correcting for multiple testing. In order to extensively investigate the effect of the magnetic field on doses at air–tissue–interfaces, we also investigated the dose to distal lung tissue, defined as any healthy lung tissue more than 5 cm from the ITV. Furthermore, we monitored the R_{50} conformity constraint, defined as follows:

$$R_{50} = \frac{V_{27.5\text{Gy}}}{\text{ITV}}$$

with $V_{27.5\text{Gy}}$ being the total volume receiving 27.5 Gy or more and the dose homogeneity index HI, calculated as:

$$\text{HI} = \frac{D_{5\%}}{D_{95\%}}$$

where $D_{5\%}$ and $D_{95\%}$ correspond to the dose level covering 5% and 95% of the ITV, respectively.

Isotoxic dose-escalated treatment plans were quantified by the maximum number of deliverable fractions. The different treatment approaches were compared with a paired t -test at a statistical significance level of $p = 0.05$. Additionally, we recorded the OAR constraint that limited further target dose escalation.

Results

Effect of MR-Linac irradiation geometry and PTV margin reduction on conventionally fractionated treatments

Statistically significant differences were found in several dose–volume metrics when comparing the conventionally fractionated treatment plans designed for the 1.5 T MR-Linac to those for the Versa HD linac (see Fig. 1). However, in all investigated cases it

was possible to design treatment plans fulfilling the planning objectives.

With regard to the lung, treatment plans with standard margins for the conventional and MR-Linac display similar mean doses (conventional linac: $14.9 \text{ Gy} \pm 0.6 \text{ Gy}$; MR-Linac: $14.9 \text{ Gy} \pm 0.5 \text{ Gy}$, $p = 0.78$). MR-Linac plans with reduced margins showed significantly lower doses ($14.3 \text{ Gy} \pm 0.6 \text{ Gy}$, $p = 0.004$). No statistically significant differences were found for the lung $V_{17\text{Gy}}$ metric (conventional linac: $29.2\% \pm 1.2\%$; MR-Linac with standard margins: $29.7\% \pm 1.4\%$, $p = 0.04$; MR-Linac with reduced margins: $29.0\% \pm 1.8\%$, $p = 0.62$). Further dosimetric analysis revealed that with both standard and reduced margins, mean dose to distal lung tissue was higher on the MR-Linac than on the conventional linac. Conversely, exposure of lung tissue close to the target was lower in MR-Linac plans with reduced margins compared to conventional linac plans. This is reflected in a decrease in the R_{50} conformity metric for the MR-Linac plans, which is exemplarily shown for one patient in Fig. 2.

We found statistically significant increases in both mean skin dose and high skin dose (skin $D_{2\%}$) in the MR-Linac plans with standard margins in comparison to the conventional linac plans (skin D_{mean} : conventional linac $4.3 \pm 1.4 \text{ Gy}$; MR-Linac: $4.7 \pm 1.5 \text{ Gy}$, $p < 0.001$; skin D_2 : conventional linac: $28.5 \pm 7.1 \text{ Gy}$; MR-Linac: $30.2 \pm 1.4 \text{ Gy}$, $p = 0.003$). However, using reduced margins the MR-Linac plans are similar to conventional linac plans for skin D_{mean} ($4.2 \pm 1.3 \text{ Gy}$, $p = 0.38$) and have a significantly lower high skin dose ($26.6 \pm 6.7 \text{ Gy}$, $p = 0.009$). We also observed reductions in oesophageal $V_{43\text{Gy}}$ and oesophageal mean dose, heart $V_{4\text{Gy}}$ and spinal canal near-maximum dose on the MR-Linac with reduced margins. However, the largest dose differences occurred in cases in which the OAR dose was substantially below the limiting planning constraint.

Potential for isotoxic dose escalation using an MR-Linac

With standard PTV margins, the potential for target dose escalation on the MR-Linac and conventional linac are similar (see Table 3). However, using reduced PTV margins, it is possible to significantly escalate target dose ($p = 0.03$). In 7 out of 10 patients, planning with reduced margins for the MR-Linac enabled additional dose escalation between 1 and 4 fractions in comparison to plans for the conventional linac. For the remaining 3 cases, 2 had equivalent dose escalation potential on the MR-Linac and conventional linac, and 1 had decreased maximum prescription level with the MR-Linac.

In 19 of 30 plans the lung dose constraint limited further dose escalation, and in the remaining 11 plans the mediastinal envelope dose constraint restricted further escalation. We found that there was more inter- than intra-patient variability in the dose

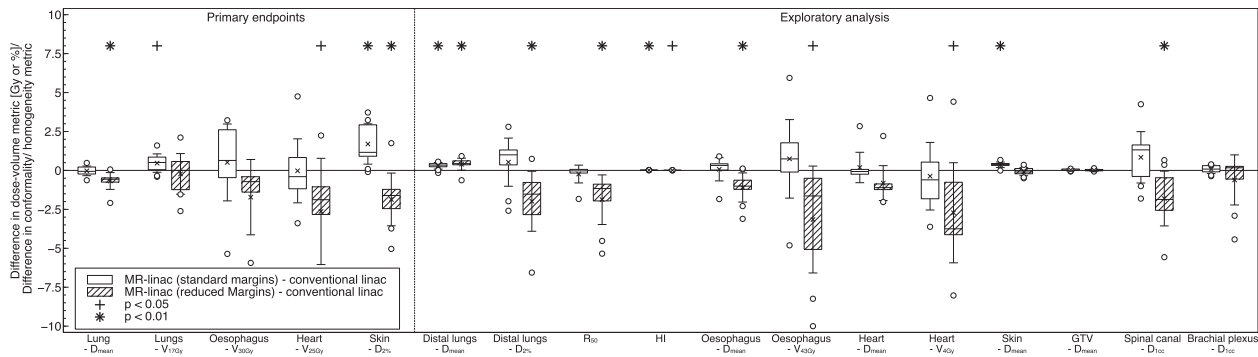


Fig. 1. Differences in the investigated dose–volume metrics between the plans designed for the MR-Linac with either standard or reduced margins and the conventional linac. Numerically positive differences mark an increase in the respective metric for the MR-Linac plans. Displayed are the first and third quartiles (boxes), medians (bands inside), average values (crosses), standard deviations (whiskers) and outliers (circles).

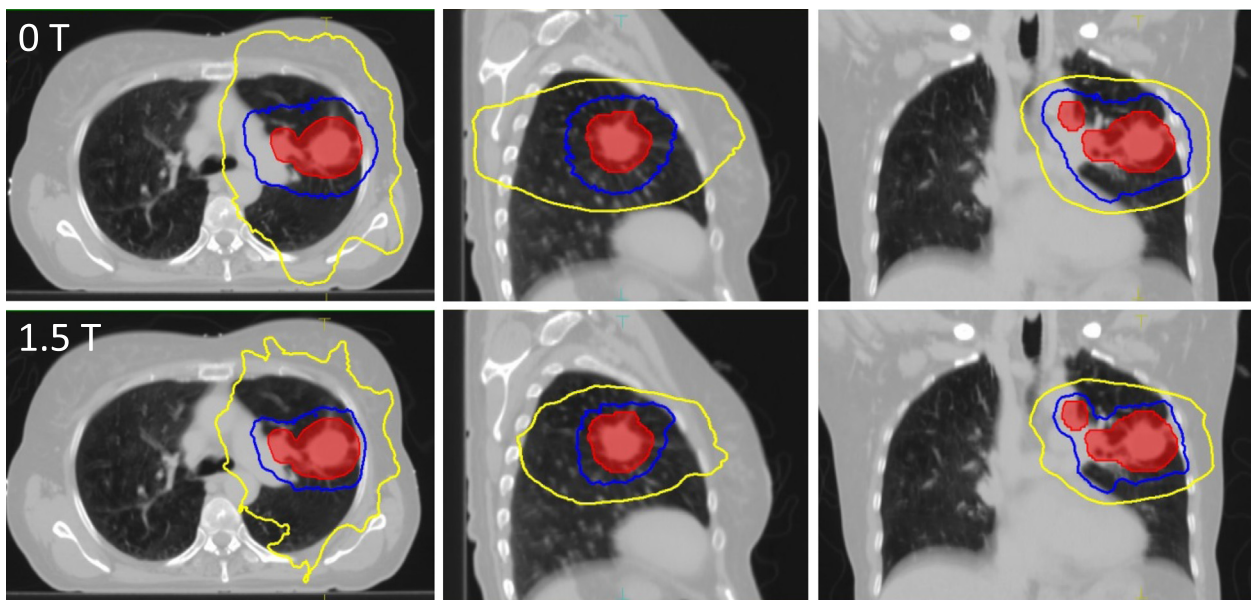


Fig. 2. Dose distribution of the conventionally fractionated treatment plans for patient 1 displayed over an axial (left), coronal (central) and sagittal (right) slice of the average phase of the 4DCT scan. Plans were created either for a conventional linac with standard margins (top row) or the MR-Linac with reduced margins (bottom row). Marked are the ITV (red) as well as the 95% (blue), 50% (yellow) isodose contours. (For interpretation of the references to colour in this figure legend, the reader is referred to the web version of this article.)

Table 3

Maximum deliverable dose for each patient when designing treatment plans following the isotoxic trial protocol without maximum target dose cap. Plans were designed for the conventional linac or the MR-Linac, with either standard or reduced PTV margins. The respective constraints limiting further target dose escalation, either mean lung dose (lung) or maximum mediastinal envelope dose (med env) are also shown. Statistical significance was measured using a paired *t*-test.

Patient number	Conventional linac (standard margins)		MR-Linac (standard margins)		MR-Linac (reduced margins)	
	CTV dose [Gy]	Limiting constraint	CTV dose [Gy]	Limiting constraint	CTV dose [Gy]	Limiting constraint
1	81.0	lung	79.2	lung	86.4	med env
2	77.4	lung	75.6	lung	79.2	lung
3	86.4	lung	81.0	lung	93.6	lung
4	79.2	med env	77.4	med env	79.2	med env
5	73.8	lung	75.6	lung	75.6	lung
6	82.8	med env	81.0	med env	81.0	med env
7	81.0	lung	81.0	lung	82.8	med env
8	73.8	med env	73.8	med env	73.8	med env
9	77.4	lung	77.4	lung	79.2	lung
10	77.4	lung	77.4	lung	81.0	lung
Mean	79.0		78.8		81.2	
Significance level			0.75		0.03	

escalation limiting constraint, which suggests that this was more dependent on patient geometry than treatment modality.

Discussion

In the first part of this study we investigated the effect of MR-Linac irradiation geometry, including the presence of a 1.5 T magnetic field, and PTV margin reduction on conventionally fractionated treatments for patients with LA NSCLC. Lung V_{17Gy} , which is derived from the V_{20Gy} metric in treatments with 2 Gy fractions, was similar for all treatment modalities. We highlight this finding as all plans were specifically optimized to minimize this dose–volume metric, and because of the importance of V_{20Gy} as indicator of pneumonitis risk [37–39]. We did observe a minor increase in dose to distal lung tissue for the MR-Linac plans in comparison to conventional linac plans. These changes are likely caused by the electron return effect at the air–tissue–interfaces of chest wall and lung, or mediastinum and lung. However, these changes are small and compared to the V_{17Gy} metric, are less likely to be clinically relevant.

The observed increase in dose to skin in the MR-Linac plans with standard margins are as expected from previous studies [25,28,40]. However, the reduction of PTV margins from approximately 7 mm to 3 mm on the MR-Linac alleviated this effect, most likely due to the smaller required size of the portal fields compensating for the electron return effect. This most likely also caused the reduction in dose to other OAR including oesophagus, heart and spinal cord. However, it has to be emphasized that the largest dose differences occurred in cases in which the OAR dose was substantially below the limiting planning constraint. For serial organs, the constraints for the optimizer were not set to reduce OAR exposure beyond a fixed threshold. Therefore, it is likely that with increased weight on these constraints further sparing could be seen at the expense of increased dose elsewhere.

In the second part of this work we investigated the influence of the MR-Linac design on isotoxic dose-escalated treatments. With standard margins the potential for target dose escalation was similar on the MR-Linac and conventional linac. A reduction in PTV margins on the MR-Linac facilitated dose escalation in 7 out of 10 patients in comparison to the Versa HD plans. Meta-analysis data in LA NSCLC suggests that a 1 Gy BED increase in radiotherapy dose results in approximately 4% relative improvement in survival based on two- and five-year survival data (median trial BED 74.67 Gy) [41]. Therefore, treating LA NSCLC on a MR-Linac may provide a survival advantage for some patients.

To our knowledge this is the first work specifically investigating the effect of MRI-guided treatment systems on radical radiotherapy for LA NSCLC patients. Wooten et al. investigated the quality of treatments delivered with the ViewRay system (ViewRay Inc., Oakwood Village, OH, USA), which combines three Cobalt-60 sources with MR imaging at 0.35 T field strength [42]. Their study includes six patients with thoracic tumours and they display the dosimetric differences for one patient with a centrally located lung tumour. Overall in these patients they found a significant increase in OAR dose (lung D_{mean} and heart D_{max}) when designing plans for the ViewRay system, particularly in the low-dose range <20 Gy, but they did not report on skin dose metrics. We planned with a 1.5 T magnetic field, and with equivalent margins observed no significant increase in lung D_{mean} or heart metrics with the MR-Linac, but did similarly observe an increase in lower doses to lung.

The margin reductions investigated in this study are one of the potential advantages to be gained by the envisioned adaptive workflow enabled by MRI-guided treatment machines. However, it is not possible to identify the entire potential benefit with our deployed methodology. In this work, we designed and evaluated

the treatment plans on the same average CT scan. This approach does not consider possible inter- or intra-fractional changes in patient anatomy, including shifting of air–tissue interface, which could have an increased impact in the presence of a magnetic field. However, another study using 4D dose reconstruction has not found a pronounced effect of moving lung–tissue interfaces in realistic patient geometries for early-stage NSCLC [28]. In the future, the ability to re-plan the treatment prior to each fraction as well as dynamically adapting the treatment to target motion based on high soft-tissue contrast MR images will likely further increase normal-tissue sparing and, in the context of isotoxic protocols, enable further target dose escalation.

In summary, this study has shown that it is feasible to design clinically acceptable treatment plans for conventionally fractionated as well as isotoxic dose-escalated radiotherapy for LA NSCLC patients with a 1.5 T MR-Linac. When incorporating the potential for PTV margin reduction facilitated by the advantageous imaging capabilities of the MR-Linac, there is scope for OAR sparing and isotoxic target dose escalation in comparison to plans generated for a conventional linac.

Acknowledgments

Research at The Institute of Cancer Research is supported by Cancer Research UK under programmes C33589/A19727, C33489/A19908 and C347/A18365. We acknowledge NHS funding to the NIHR Biomedical Research Centre at The Royal Marsden and The Institute of Cancer Research.

Conflict of interest

The Institute of Cancer Research is part of the Elekta MR-Linac Consortium and we acknowledge financial and technical support from Elekta AB under a research agreement. However, the sponsors had no part in the design or execution of the study.

Appendix A. Supplementary data

Supplementary data associated with this article can be found, in the online version, at <https://doi.org/10.1016/j.radonc.2017.09.009>.

References

- [1] Aupérin A, Le Péchoux C, Rolland E, et al. Meta-analysis of concomitant versus sequential radiochemotherapy in locally advanced non-small-cell lung cancer. *J Clin Oncol* 2010;28:2181–90.
- [2] Machtay M, Paulus R, Moughan J, et al. Defining local-regional control and its importance in locally advanced non-small cell lung carcinoma. *J Thorac Oncol* 2012;7:716–22.
- [3] Christodoulou M, Bayman N, McCloskey P, Rowbottom C, Faivre-Finn C. New radiotherapy approaches in locally advanced non-small cell lung cancer. *Eur J Cancer* 2014;50:525–34.
- [4] Onishi H, Shirato H, Nagata Y, et al. Hypofractionated stereotactic radiotherapy (HypoFRT) for stage I non-small cell lung cancer: updated results of 257 patients in a Japanese multi-institutional study. *J Thoracic Oncol* 2007;2:S94–S100.
- [5] Faivre-Finn C. Dose escalation in lung cancer: have we gone full circle? *Lancet Oncol* 2015;16:125–7.
- [6] Bradley JD, Paulus R, Komaki R, et al. Standard-dose versus high-dose conformal radiotherapy with concurrent and consolidation carboplatin plus paclitaxel with or without cetuximab for patients with stage IIIA or IIIB non-small-cell lung cancer (RTOG 0617): a randomised, two-by-two factorial p. *Lancet Oncol* 2015;16:187–99.
- [7] De Ruyscher D, Van Baardwijk A, Steevens J, et al. Individualised isotoxic accelerated radiotherapy and chemotherapy are associated with improved long-term survival of patients with stage III NSCLC: A prospective population-based study. *Radiother Oncol* 2012;102:228–33.
- [8] Landau DB, Hughes L, Baker A, et al. IDEAL-CRT: A phase I/II trial of isotoxic dose-escalated radiotherapy and concurrent chemotherapy in patients with stage II/III non-small cell lung cancer. *Int J Radiat Oncol Biol Phys*. 2016;95:1367–77.

- [9] van Baardwijk A, Reymen B, Wanders S, et al. Mature results of a phase II trial on individualised accelerated radiotherapy based on normal tissue constraints in concurrent chemo-radiation for stage III non-small cell lung cancer. *Eur J Cancer* (Oxford, England: 1990) 2012;48:2339–46.
- [10] van Baardwijk A, Wanders S, Boersma L, et al. Mature results of an individualized radiation dose prescription study based on normal tissue constraints in stages I to III non-small-cell lung cancer. *J Clin Oncol* 2010;28:1380–6.
- [11] Warren M, Webster G, Ryder D, Rowbottom C, Faivre-Finn C. An isotoxic planning comparison study for stage II-III non-small cell lung cancer: is intensity-modulated radiotherapy the answer? *Clin Oncol* 2014;26:461–7.
- [12] Kwint M, Conijn S, Schaake E, et al. Intra thoracic anatomical changes in lung cancer patients during the course of radiotherapy. *Radiother Oncol* 2014;113:392–7.
- [13] Kataria T, Gupta D, Bisht SS, et al. Adaptive radiotherapy in lung cancer: dosimetric benefits and clinical outcome. *Br J Radiol* 2014;1038:20130643.
- [14] Fallone BG, Murray B, Rathee S, et al. First MR images obtained during megavoltage photon irradiation from a prototype integrated linac-MR system. *Med Phys* 2009;36:2084–8.
- [15] Keall PJ, Barton M, Crozier S, on behalf of the Australian MRI-Linac Program including contributors from Ingham Institute Illawarra Cancer Care Centre Liverpool Hospital Stanford University Universities of Newcastle Queensland Sydney Western Sydney and Wollongong. The Australian magnetic resonance imaging-linac program. *Semin Radiat Oncol* 2014;24:203–6.
- [16] Raaymakers BW, Lagendijk JJ, Overweg J, et al. Integrating a 1.5 T MRI scanner with a 6 MV accelerator: proof of concept. *Phys Med Biol* 2009;54:N229–37.
- [17] Mutic S, Dempsey JF. The ViewRay system: magnetic resonance-guided and controlled radiotherapy. *Semin Radiat Oncol* 2014;24:196–9.
- [18] Aoyama H, Shirato H, Nishioka T, et al. Magnetic resonance imaging system for three-dimensional conformal radiotherapy and its impact on gross tumor volume delineation of central nervous system tumors. *Int J Radiat Oncol Biol Phys* 2001;50:821–7.
- [19] Yeung AR, Vargas CE, Falchook A, et al. Dose-volume differences for computed tomography and magnetic resonance imaging segmentation and planning for proton prostate cancer therapy. *Int J Radiat Oncol Biol Phys* 2008;72:1426–33.
- [20] Chuter R, Prestwich R, Bird D, et al. The use of deformable image registration to integrate diagnostic MRI into the radiotherapy planning pathway for head and neck cancer. *Radiother Oncol* 2017;122:229–35.
- [21] Raaymakers BW, Raaijmakers AJE, Kotte ANTJ, Jette D, Lagendijk JJW. Integrating a MRI scanner with a 6 MV radiotherapy accelerator: dose deposition in a transverse magnetic field. *Phys Med Biol* 2004;49:4109–18.
- [22] Raaijmakers AJ, Raaymakers BW, Lagendijk JJ. Experimental verification of magnetic field dose effects for the MRI-accelerator. *Phys Med Biol* 2007;52:4283–91.
- [23] Raaijmakers AJ, Raaymakers BW, Lagendijk JJ. Integrating a MRI scanner with a 6 MV radiotherapy accelerator: dose increase at tissue-air interfaces in a lateral magnetic field due to returning electrons. *Phys Med Biol* 2005;50:1363–76.
- [24] Kirkby C, Murray B, Rathee S, Fallone BG. Lung dosimetry in a linac-MRI radiotherapy unit with a longitudinal magnetic field. *Med Phys* 2010;37:4722–32.
- [25] Yang YM, Geurts M, Smilowitz JB, Sterpin E, Bednarz BP. Monte Carlo simulations of patient dose perturbations in rotational-type radiotherapy due to a transverse magnetic field: a tomotherapy investigation. *Med Phys* 2015;42:715–25.
- [26] Merna C, Rwigema JC, Cao M, et al. A treatment planning comparison between modulated tri-cobalt-60 teletherapy and linear accelerator-based stereotactic body radiotherapy for central early-stage non-small cell lung cancer. *Med Dosim* 2016;41:87–91.
- [27] Oborn BM, Ge Y, Hardcastle N, Metcalfe PE, Keall PJ. Dose enhancement in radiotherapy of small lung tumors using inline magnetic fields: a Monte Carlo based planning study. *Med Phys* 2016;43:368.
- [28] Menten MJ, Fast MF, Nill S, Kamerling CP, McDonald F, Oelfke U. Lung stereotactic body radiotherapy with an MR-linac - Quantifying the impact of the magnetic field and real-time tumor tracking. *Radiother Oncol* 2016;119:461–6.
- [29] Park JM, Park SY, Kim HJ, Wu HG, Carlson J, Kim JI. A comparative planning study for lung SABR between tri-Co-60 magnetic resonance image guided radiation therapy system and volumetric modulated arc therapy. *Radiother Oncol* 2016;120:279–85.
- [30] Acharya S, Fischer-Valuck BW, Kashani R, et al. Online magnetic resonance image guided adaptive radiation therapy: first clinical applications. *Int J Radiat Oncol Biol Phys* 2016;94:394–403.
- [31] van Herk M, Remeijer P, Rasch C, Lebesque JV. The probability of correct target dosage: dose-population histograms for deriving treatment margins in radiotherapy. *Int J Radiat Oncol Biol Phys* 2000;47:1121–35.
- [32] Guckenberger M, Krieger T, Richter A, et al. Potential of image-guidance, gating and real-time tracking to improve accuracy in pulmonary stereotactic body radiotherapy. *Radiother Oncol* 2009;91:288–95.
- [33] Haslett K, Franks K, Hanna GG, et al. Protocol for the isotoxic intensity modulated radiotherapy (IMRT) in stage III non-small cell lung cancer (NSCLC): a feasibility study. *BMJ Open* 2016;6:e010457.
- [34] Hissoiny S, Ozell Bt, Bouchard H, Després P. GPUMCD: a new GPU-oriented Monte Carlo dose calculation platform. *Med Phys* 2011;38:754–64.
- [35] Lilliefors HW. On the Kolmogorov-Smirnov test for normality with mean and variance unknown. *J Am Stat Assoc* 1967;62:399–402.
- [36] Dunn OJ. Multiple comparisons among means. *J Am Stat Assoc* 1961;56:52–64.
- [37] Marks LB, Bentzen SM, Deasy JO, et al. Radiation dose-volume effects in the lung. *Int J Radiat Oncol Biol Phys* 2010;76:S70–6.
- [38] Palma DA, Senan S, Tsujino K, et al. Predicting radiation pneumonitis after chemoradiation therapy for lung cancer: an international individual patient data meta-analysis. *Int J Radiat Oncol Biol Phys* 2013;85:444–50.
- [39] Chun SG, Hu C, Choy H, et al. Impact of intensity-modulated radiation therapy technique for locally advanced non-small-cell lung cancer: a secondary analysis of the NRG oncology RTOG 0617 randomized clinical trial. *J Clin Oncol* 2017;35:56–62.
- [40] van Heijst TC, den Hartogh MD, Lagendijk JJ, van den Bongard HJ, van Asselen B. MR-guided breast radiotherapy: feasibility and magnetic-field impact on skin dose. *Phys Med Biol* 2013;58:5917–30.
- [41] Machtay M, Bae K, Movsas B, et al. Higher biologically effective dose of radiotherapy is associated with improved outcomes for locally advanced non-small cell lung carcinoma treated with chemoradiation: an analysis of the Radiation Therapy Oncology Group. *Int J Radiat Oncol Biol Phys* 2012;82:425–34.
- [42] Wooten HO, Green O, Yang M, et al. Quality of intensity modulated radiation therapy treatment plans using a 60Co magnetic resonance image guidance radiation therapy system. *Int J Radiat Oncol Biol Phys* 2015;92:771–8.